EFFECTS OF POURING TECHNIQUE ON ORIENTATION OF STEEL AND SYNTHETIC MACROFIBRES IN FIBRE-REINFORCED CONCRETE

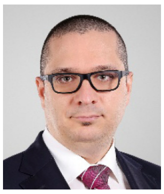

Károly Péter Juhász

https://doi.org/10.32970/CS.2020.1.1

Fibre-reinforced concrete is a short-fibre composite material, whose properties are significantly dependent on the orientation of the mixed fibres. As a starting point, the fibres are assumed to be uniformly distributed and have a uniform orientation. However, in reality, they have a non-uniform distribution owing to various factors. Such deviations in the orientation may have a significant effect on the material parameters, both favourable and unfavourable. In this study, the orientation factors determined based on the mixing models reported in the literature are compared with the results of experimental tests performed in the laboratory, and the effects of the formwork and the pouring methods used on the orientation of both steel and synthetic macrofibres are investigated. Based on the results of the study, the orientation of the fibres (both, steel and macro synthetic) significantly depends on the pouring method, which considerably influences the material parameters of fibre-reinforced concrete.

Keywords: fibre reinforced concrete, mixing model, steel fibre, synthetic macro fibre

1. INTRODUCTION

Fibres mixed in concrete, which is a quasibrittle material, can improve several properties such as the fracture energy and ductility, which must be taken into account during the design stage (Gopalaratnam et al., 1991; Balaguru and Shah, 1992). The residual flexural strength of materials is measured using the three-point or four-point bending beam test, such as the EN 14651 (EN 14651, 2007) or ASTM C-1609 test (ASTM C-1609, 2019), respectively. The size and cross-section of the beam used depends on the standard employed. However, the most common cross-sectional dimensions are 150 × 150 mm^2. The residual flexural strength primarily depends on the number and locations of the fibres on the crack surfaces. However, other factors, such as the fibre content (i.e., number of fibres added), geometry of the fibres, and the homogeneity of the mix also have an effect. The number of fibres intersecting the cross-section is a key parameter. Romualdi and Mandel (1964) and later Naaman (1972) proposed expressions for determining this number while Krenchel (1975) introduced the orientation factor to characterize the fibre orientation. Assuming ideal mixing, the orientation factor should be 0.5 (Stroeven, 1978).

However, several factors can affect the fibre orientation, and the most important one is probably the wall effect. There have been several studies on the determination of the factors that affect the fibre orientation, including the wall effect (Kameswara Rao, 1979; Stroeven 1991, 1999; Soroushian and Lee, 1990; Hoy, 1998; Kooiman, 2000; Dupont and Vandewalle, 2005; Lee, Cho and Vecchio, 2011; Ng, Foster and Htut, 2012). During the vibration and compaction of concrete, the fibre orientation will change (Soroushian and Lee, 1990; Edgington and Hannant, 1972; Stroeven, 1979; Toutanji and Bayasi, 1998; Stahli, Custer, and van Mier, 2008). Zerbino et al. (2012) investigated the orientation of steel fibres in self-compacted concrete elements, such as slabs, walls, and beams, and so did Sarmiento et al. (2012), who compared the results of numerical calculations with those of tests performed on fibre-reinforced concrete (FRC) beams. The wall effect in the case of synthetic macrofibres is different from that for steel fibres because of their higher stiffness; steel fibers rotate when they come into contact with the wall while synthetic ones bend. In contrast, Oh, Kim, and Choi (2007) did not take this effect into account in their model, while Alberti (2017) and Juhász (2018a, 2018b) suggested a method for considering it during modelling.

Because of these effects, the orientation of the fibres will not be uniform. Thus, the number of fibres that intersect the cross-section will also change. In the case of beam tests performed on a relatively small cross-sectional reference area, the residual flexural strength will exhibit a wide distribution, owing to which the values of the designed and actual parameters will be lower than required (Bernard, 2013). This can lead to exaggerated safety assessment results and uneconomical designs. Thus, the number of fibres intersecting the cross-section is an important parameter that must be determined with precision. However, few standards and guidelines exist on how to do so (Juhász, 2019).

The Italian CNR-DT guidelines (2006) consider the orientation in their introduction, drawing attention to the fact that the orientation of the fibres depends primarily on the pouring method used and has a determining effect on the properties of the concrete. However, they do not take it into account while evaluating the material parameters. In contrast, the RILEM TC-162 (Vandewalle et al., 2003) guidelines do not consider the orientation at all. On the other hand, the Austrian ÖVBB Richtlinie Faserbeton guidelines (2008) for hybrid materials (FRC with conventional steel bar reinforcement) and slab-type elements (those with $b > 5h$ and $bh > 1.0$ m^2, where b is the width and h is the height of the elements) suggest that the residual flexural strength increases by a factor of $\eta = 1.4$. The reason for this increase is not discussed. However, based on the geometrical parameters, it is likely that this increase is due to the fibre orientation. Section 6.5.7 of the fib Model Code (2013) is devoted to the effects of the fibre orientation. Factor K is defined as the orientation factor, and its value is 1.0 in general. The code also states that whether the orientation of the fibres is uniform or not must be verified experimentally. If the orientation is favourable, its effects may be taken into consideration; in case of unfavourable orientation, the orientation factor must be applied in the calculation. However, no methods for doing so are suggested.

In this paper, the various analytical mixing models and the corresponding orientation factors reported in the literature are reviewed. The effects of these orientation factors are compared with the results of experimental tests. These tests were performed on FRC beams produced using different pouring techniques and different types of fibres (steel and synthetic macrofibres), and the number of fibres intersecting the cross-section and the corresponding orientation factors are determined. Finally, the effects of the different pouring methods are compared based on the results of numerical calculations and experimental tests.

2. ANALYTICAL MIXING MODELS

The number of fibres that intersect the unit-area cross-section is the basis for most material models that consider the fibres discretely. These model include the variable engagement model (Voo and Foster, 2003), the diverse embedment model (Lee, Cho, and Vecchio, 2011), the simplified diverse embedment model (Lee, Cho, and Vecchio, 2013), and the hybrid diverse embedment model (Chasioti, 2017). The orientation of the fibres is also a relevant parameter for evaluating experimental results. On the one hand, the quality of the mixing can be determined based on the fibre orientation (Dupont and Vandewalle, 2005), while on the other hand, the effect of the nonuniform distribution of the fibres on crack formation in the cross-section can also be considered (Juhász, 2013; Juhász, 2015). Numerous studies have examined the impact of mixing on the experimental results in the case of different types of elements (Zerbino et al., 2012; Sarmiento et al., 2012).

2.1. Method proposed by Romualdi and Mandel (1964)

Fibres parallel or nearly parallel to the tensile stress are effective in controlling cracks. Thus, corrections must be made for the fibres that are not oriented as desired. Romualdi and Mandel (1964) assumed that the ratio of the average of the projected lengths in a given direction to the total length is a suitable correction measure. The projection of a fibre in the x-direction such that the origin is the midpoint of the fibre and

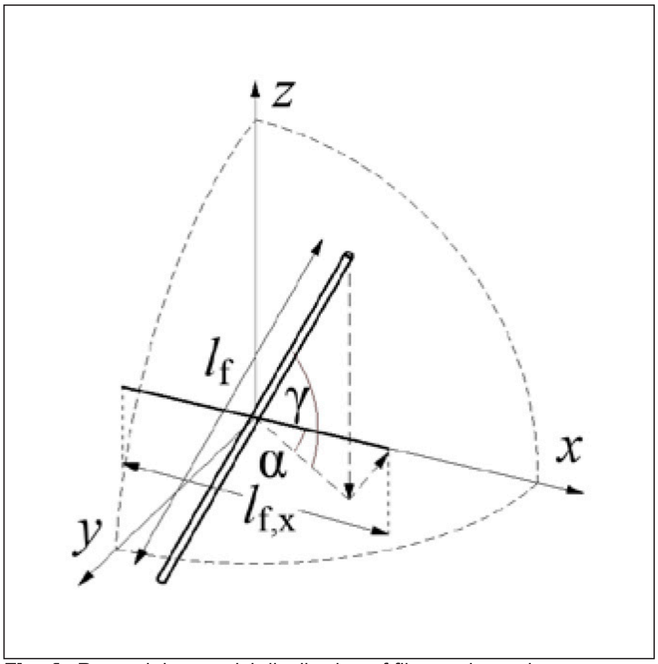

Fig. 1: *Determining spatial distribution of fibres using polar coordinates α and γ*

the orientation is defined using polar coordinates α and γ can be given as follows:

$$l_{f,x} = l_f \cos\alpha \cos\gamma \tag{1}$$

where l_f is the length of the fibre and α and γ are the polar coordinates, as shown in *Fig. 1*.

Based on this, if a midpoint and length l_f as projected on the x-axis are given, along with a uniform distribution of α and γ , the average length of the fibres will be given by

$$l_{f,x,m,1} = \frac{\int_0^{\frac{\pi}{2}}\int_0^{\frac{\pi}{2}} l_f \cos\alpha \cos\gamma \, d\alpha \, d\gamma}{\left(\frac{\pi}{2}\right)^2} = 0.405 l_f \tag{2}$$

Romualdi and Mandel derived the number of fibres intersecting the unit-area cross-section from the average distance of the midpoints of the fibres, as follows:

$$n = \frac{l_{f,x,m,1} N}{V} = 0.405 l_f \frac{N}{V} \tag{3}$$

where n is the number of fibres intersecting the unit-area cross section [/m^2] and N is the total number of fibres in volume V.

2.2. Method proposed by Naaman (1972)

Naaman (1972) determined the number of fibres intersecting the cross-section based on a probability analysis. Consider a fibre whose midpoint lies on the x-axis (*Fig. 2*):

If the midpoint of the fibre is located at a distance smaller than $0.5 l_f$, then the fibre will intersect the crack plane. The probability of this is the quotient of the surface areas of spherical cap S_i and half-sphere S drawn around the midpoint

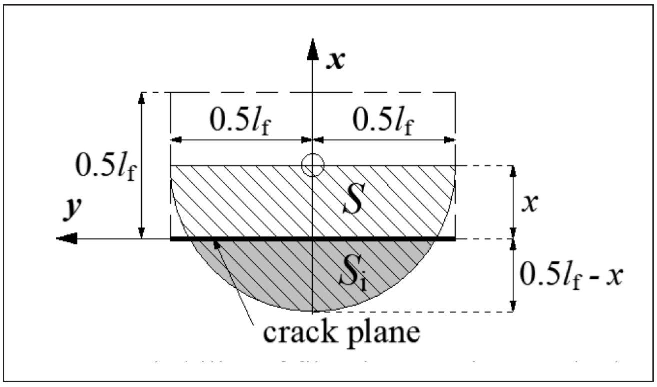

Fig. 2: Probability of fibre intersecting crack plane

of the fibre, as shown in *Fig. 2*.

$$q_{\text{Naaman}} = \frac{S_i}{S} = \frac{0.5l_f - x}{0.5l_f} = 1 - \frac{2x}{l_f} \tag{4}$$

Considering the unit volume on both sides of the crack plane, the number of fibres intersecting the unit-area cross-section will be similar to that obtained using the expression for a uniform distribution in a sphere (Eq. 3):

$$n = 2\int_0^{\frac{l_f}{2}} \left(1 - \frac{2x}{l_f}\right)\frac{N}{V}dx = \frac{N}{V}2\int_0^{\frac{l_f}{2}}\left(1 - \frac{2x}{l_f}\right)dx = \frac{N}{V}0.5l_f \tag{5}$$

2.3. Orientation factor proposed by Krenchel (1975)

Let us assume that, in the ideal state, each fibre is perpendicular to the crack plane. Then, in the current case, each fibre will be aligned along the *x*-axis. Based on the volume fraction of the fibres, V_f, which is the weight of the fibres in concrete [kg/m^3] divided by the bulk density of the fibres [kg/m^3], and the cross-sectional area of a single fibre, A_f, the number of fibres intersecting cross-section A can be determined as:

$$n_i = \frac{V_f}{A_f}A \tag{6}$$

where n_i [-] represents the ideal number of fibres in cross-section A.

Given that the orientation of the fibres would not be perpendicular to the crack plane in reality, Krenchel (1975) introduced the orientation factor:

$$\theta_{\text{Krenchel}} = \frac{n_a}{n_i} = n_a\frac{A_f}{V_f A} \tag{7}$$

where n_a is the number [pc] of fibres intersecting cross-section A, as determined experimentally by counting the fibres in a cracked surface or sliced section.

Thus, it can be seen that the orientation factor proposed by Krenchel (1975) is similar to the factor for modifying the fibre length used by Romualdi and Mandel (1964) and Naaman (1972), whose value is 0.5 in case the fibre distribution is uniform (Stroeven, 1978).

2.4. Orientation factors suggested by Dupont and Vandewalle and proposed model

Dupont and Vandewalle (2005) used the cross-section dimensions recommended in RILEM TC-162 (Vandewalle et al., 2003) and investigated the influence of the wall effect on the orientation factors herein. They divided the cross-section of a beam into three zones in order to consider the effects of the formwork used: 1: undisturbed zone, 2: disturbed zone–one side of the mould, and 3: disturbed zone–two sides of the mould (corner) (Figure 3a). Steel fibres are rigid and thus would rotate when they come into contact with the formwork. The orientation factors proposed by Dupont and Vandewalle were subsequently modified by Juhász (2018b), who took into account the differences between rigid (steel) and flexible (synthetic) fibres. The different orientation factors are shown in *Fig. 3*.

Fig. 3: Cross-section zones and orientation factors proposed by (a) Dupont and Vandewalle for steel fibres and Juhász for (b) steel and (c) synthetic fibres.

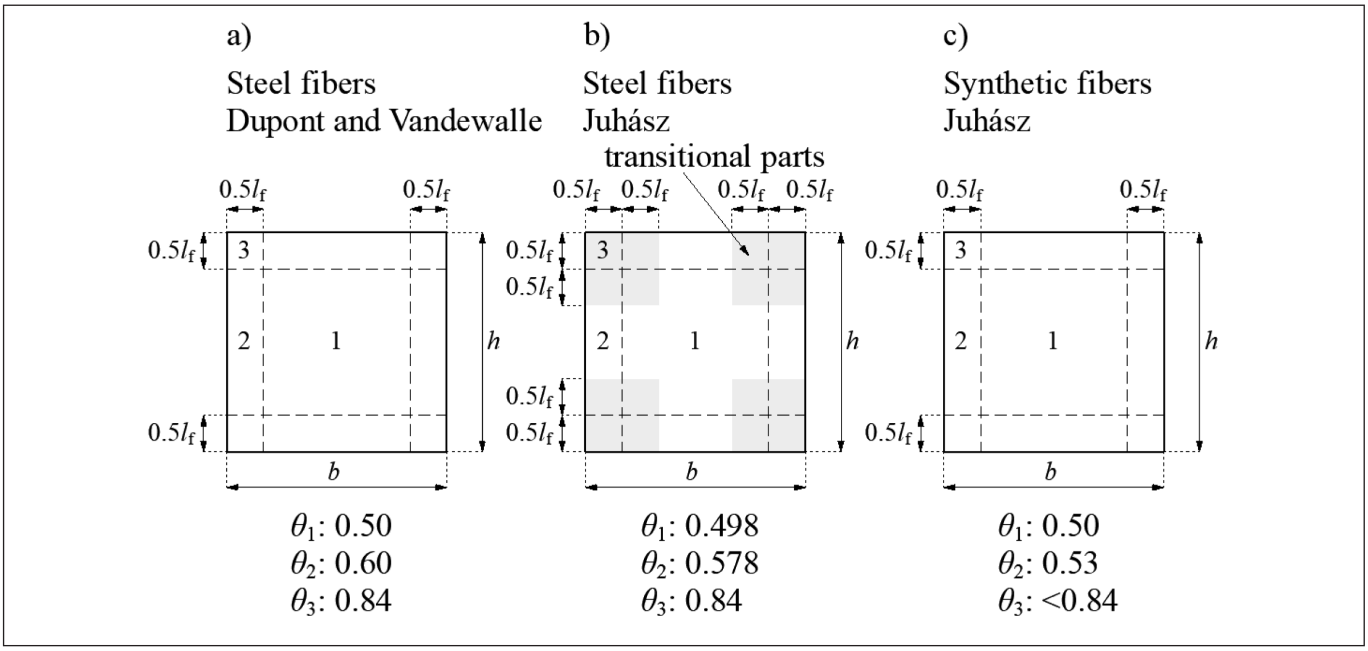

The orientation factor for the entire cross-section can be calculated from the weighted mean:

$$\theta_T = \sum_{i=1}^{n} \frac{A_i}{A} \theta_i \tag{8}$$

where θ_T is the orientation factor of the entire cross-section, A_i is the area of cross-section zone *i*, *A* is the area of the entire cross-section, and θ_i is the orientation factor of zone *i*.

In the rest of the study, the orientation factors proposed by Juhász (2018b) for steel and synthetic fibres (see Figures 3(b) and (c)) are used.

3. LABORATORY TESTS

FRC beams with steel and synthetic macrofibres were produced using different pouring techniques. The contents of the two types of fibers were kept the same to allow for a comparison of the numbers of fibres intersecting the beam cross-sections. In the case of a high steel fibre content, the fibres would have a significant effect on each other's movement; this, in turn, would affect their orientation as well (Juhász, 2018b; Kang et al., 2011; Czoboly, 2016). Thus, their content was limited to ~30 kg/m^3. The composition of the concrete mix is listed in *Table 1*, while the fibre types used and their properties are listed in *Table 2*. The water/cement ratio was kept at 0.5, and the consistency of the concrete was F5.

Table 1: Composition of concrete mix

Component	Quantity (kg/m^3)
Aggregate (4–8 mm)	629
Sand (0–4)	997
Microsilica	40
Cement (CEM I 42,5 R)	400
Water	200
Superplasticizer (Mapei SR1)	3

Table 2: Material properties of fibres used

Property	Steel fibres (ST)	Synthetic fibres (SY)
Base material	Steel	Polypropylene
Tensile strength [MPa]	700	550
Elastic modulus [GPa]	200	10
Diameter/length [mm]	1/50	0.7/48
Anchorage	Hooked end	Continuous embossing
Fibres/kg	3 181	35 714
Content [kg/m^3]	33.73	3
Content [fibre/m^3]	107 346	107 346

The dimensions of the beams were 150 × 150 × 1000 mm^3, and they were produced using two different pouring methods. The first method (P1) was the one recommended in RILEM TC-162 (Vandewalle et al., 2003), while in the case of the second method (P2), the formwork was tilted at an angle of 45° during pouring and then set in the vertical position until the concrete had hardened. In addition, for the two pouring methods, the flow directions of the poured concrete were also different. For P1, it was perpendicular to the longitudinal axis of the beam while for P2, it was parallel to the axis. The two flow directions are denoted by arrows in *Fig. 4*. The formworks used were made from plastic-covered plywood, and form

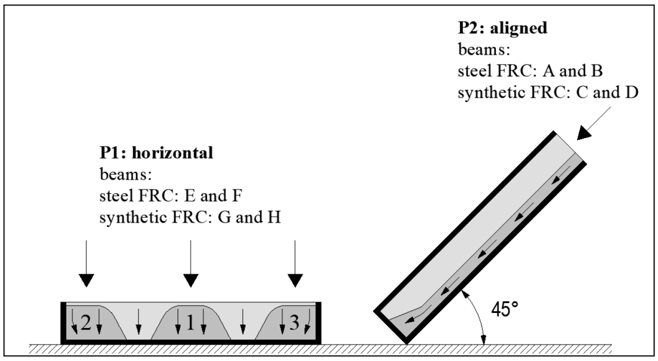

Fig. 4: Pouring methods P1 (formwork was horizontal) and P2 (formwork was inclined).

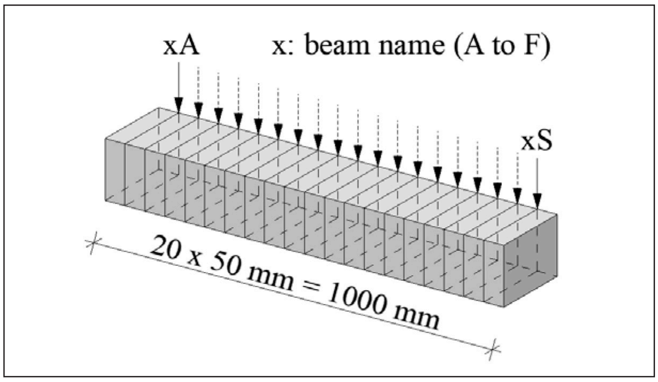

Fig. 5: Investigated cross-sections.

oil was applied prior to pouring of the concrete. In the case of pouring method P1, the formwork was open on one side along its length, while in the case of P2, the formwork was open at the endplate. After the pouring process, there was no need to subject the formworks to vibrations for compaction.

After the hardening of the concrete, the beams were cut into 50-mm slices, as shown in *Fig. 5*, and their surfaces were investigated.

Fibres could be seen intersecting the cross-sections in the case of all the beams. As stated previously, the cross-sections were divided into different zones (*see Fig. 3*), and the numbers of intersecting fibres in these zones were determined. The research matrix is shown in *Table 3*. A typical cross-section of a steel-fibre-reinforced concrete beam is shown in *Fig. 6*.

Table 3: Research matrix

Fibre type	Pouring method	Beam label	Section labels
Steel	(P1) Hori-zontal	E, F	EA…ES; FA…FS
Steel	(P2) Inclined	A, B	AA…AS; BA…BS
Synthetic macrofibres	(P1) Horizontal	G, H	GA…GS; HA…HS
Synthetic macrofibres	(P2) Inclined	C, D	CA…CS; DA…DS

4. RESULTS

The results of the statistical analysis are listed in *Table 4*. During the analysis, the mean value of the number of intersecting fibres, its standard deviation, and coefficient of variation (CV) were determined. Then, the sample averages were analysed using Tukey's biweight M-estimator and the Shapiro-Wilk normality test in order to determine whether the data were normally distributed.

The histograms of the numbers of fibres intersecting the

Table 4: Results of statistical analysis

Sample name	Mean value	SD	CV (%)	M-estimator[1]	Normality[2]
P1-ST-Z1	33.526	15.485	46.19	29.264	0.011
P1-ST-Z2	31.894	10.159	31.85	31.526	**0.673**
P1-ST-Z3	5.907	2.683	45.42	5.484	**0.097**
P1-ST-TOT	71.328	23.102	32.39	67.756	0.045
P2-ST-Z1	24.842	11.117	44.75	21.052	0.000
P2-ST-Z2	18.618	8.306	44.62	16.763	0.003
P2-ST-Z3	3.407	1.930	56.65	3.281	**0.149**
P2-ST-TOT	46.868	16.542	35.29	40.515	0.001
P1-SY-Z1	37.157	8.958	24.11	35.859	0.033
P1-SY-Z2	32.671	6.237	19.09	34.310	0.02
P1-SY-Z3	8.000	4.170	52.13	6.875	0.001
P1-SY-TOT	77.828	11.493	14.77	76.661	**0.211**
P2-SY-Z1	16.657	7.213	43.30	16.035	**0.27**
P2-SY-Z2	23.921	6.085	25.44	23.613	**0.96**
P2-SY-Z3	6.263	2.409	38.48	6.059	**0.534**
P2-SY-TOT	46.842	11.336	24.20	47.194	**0.309**

1: Tukey´s biweight M-estimator
2: Shapiro-Wilk test of normality (null hypothesis accepted if $p > 0.05$; shown in bold)

Table 5: Comparison of test and analytical results

Steel FRC beams						
Pouring method	Zone	Test		Analytical		
		θ mean	θ M-est	θ	Difference mean	Difference M-est
P1	Z1	0.625	0.545	0.498	–20.27	–8.66
	Z2	0.594	0.587	0.578	–2.73	–1.60
	Z3	0.440	0.409	0.84	+90.78	+105.53
	TOT	0.591	0.561	0.57	–3.50	+1.59
P2	Z1	0.463	0.392	0.498	+7.60	+26.97
	Z2	0.347	0.312	0.578	+66.63	+85.07
	Z3	0.254	0.245	0.84	+230.83	+243.53
	TOT	0.388	0.335	0.57	+46.87	+69.90
Total	Z1	0.544	-	0.498	–8.41	-
	Z2	0.471	-	0.578	+22.83	-
	Z3	0.347	-	0.84	+142.01	-
	TOT	0.489	-	0.57	+16.48	-
Synthetic FRC beams						
Pouring method	Zone	Test		Analytical		
		θ mean	θ M-est	θ	Difference mean	Difference M-est
P1	Z1	0.693	0.668	0.5	–27.86	–25.16
	Z2	0.648	0.639	0.53	–18.15	–17.09
	Z3	0.674	0.512	0.84	+24.65	+63.95
	TOT	0.671	0.635	0.55	–18.07	–13.36
P2	Z1	0.311	0.299	0.5	+60.92	+67.36
	Z2	0.474	0.440	0.53	+11.79	+20.47
	Z3	0.528	0.452	0.84	+59.22	+86.03
	TOT	0.404	0.391	0.55	+36.12	+40.74
Total	Z1	0.502	-	0.5	–0.38	-
	Z2	0.561	-	0.53	–5.50	-
	Z3	0.601	-	0.84	+39.83	-
	TOT	0.538	-	0.55	+2.29	-

various cross-section zones as well as for the entire cross-section and the corresponding distributions are shown in *Fig. 7*. The data for the different pouring methods are shown in the same graphs for ease of comparison. The distribution was narrower in the case of larger surfaces. Thus, the CV was the smallest in the case of the entire cross-section. The distribution

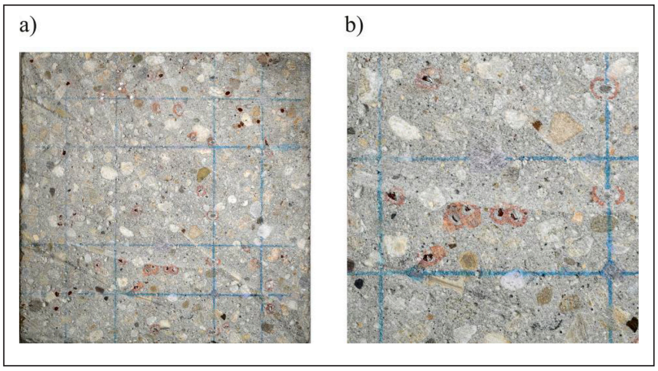

Fig. 6: Typical cross-section of steel FRC beam: (a) complete cross-section with various zones marked and (b) higher-magnification image of cross-section.

curves that passed the normality test are represented by solid lines while those that did not are represented by dashed lines.

The orientation factors were calculated from the mean values and the results of the M-estimator test. The values of the orientation factors were then compared with the analytical results. The orientation factors for all the beams (those fabricated using both the P1 method and the P2 method) were also determined and compared with the analytical results. These results are listed in *Table 5*.

Near the end plate of the formwork, the flow direction of the concrete changes, and the wall effect becomes more pronounced. To highlight this, the number of fibres intersecting the cross-section are shown along the longitudinal

Fig. 7: Histograms and corresponding distribution curves for numbers of fibres intersecting various cross-section zones and entire cross-section in case of steel and synthetic macrofibres (black columns and bold distribution curve: P1 (horizontal) pouring method and grey columns and thin distribution curves: P2 (inclined) pouring method).

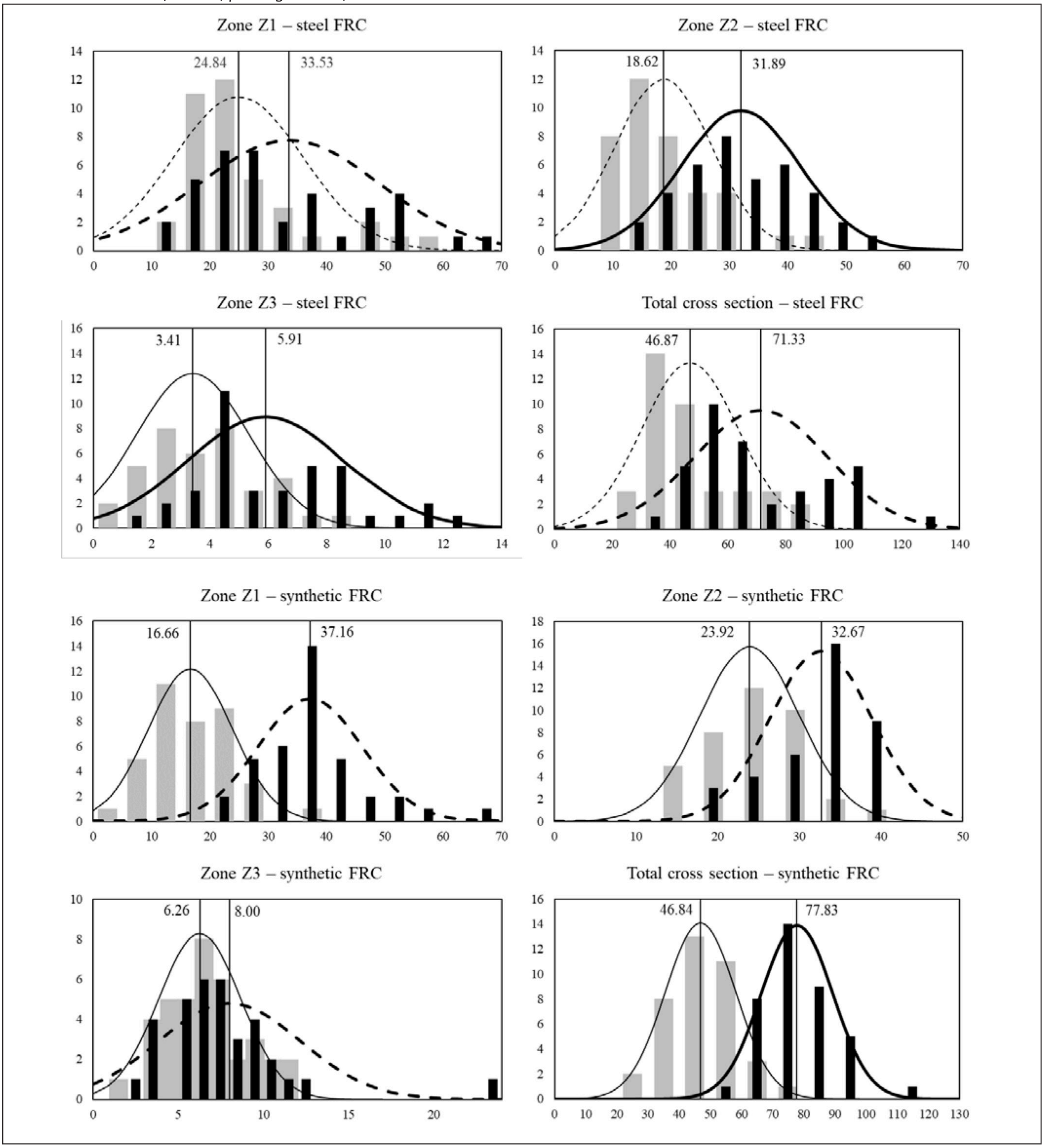

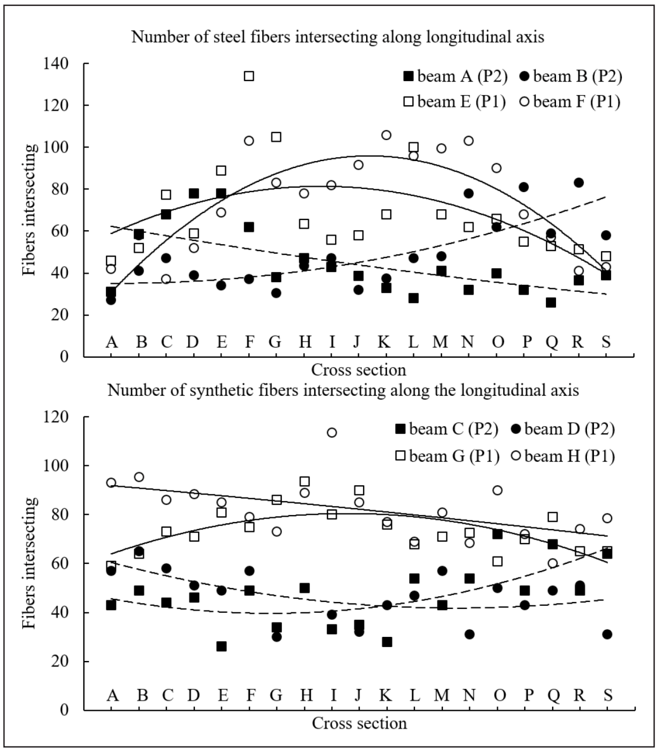

Fig. 8: Changes in number of fibres intersecting cross-section along longitudinal axis of beams (solid line: pouring method P1 and dashed line: pouring method P2).

axis of the beam in *Fig. 8*. The results for the two pouring methods and two fibre types are shown in the same diagrams. A second-order polynomial regression curve was fitted to the data to illustrate the changes in the number of fibres along the longitudinal axis.

5. DISCUSSION

It can be seen clearly that the choice of the pouring method used has a significant effect on the number of fibres intersecting the cross-sections. This was true for both steel and synthetic macrofibres. The numbers of steel and synthetic fibres that intersected the cross-sections of the beams formed by method P2 were 34% and 39% lower, respectively, that those in the case of the beams formed using method P1. A similar difference was also observed in the case of the different cross-section zones as well as between the zones and the total cross-section. Therefore, it can be assumed that the pouring method has a determining effect on the orientation of the incorporated fibres.

The flow of the concrete can explain these differences. In the flowing concrete matrix, the fibers are oriented perpendicular to the direction of the flow (Toutanji and Bayasi, 1998; Stahli, Custer, and van Mier, 2008; Stahli, and van Mier, 2007). In the case of the horizontal pouring method (P1), the flow direction of the concrete is vertical. Thus, the orientation of the fibres is horizontal. The vibration of these beams may cause the fibres to become even more aligned horizontally (Soroushian and Lee, 1990; Toutanji and Bayasi, 1998; Barragán et al., 2000). In contrast, in the case of the inclined pouring method (P2), the concrete flow direction is parallel to the longitudinal axis of the beam. Thus, the orientation of the fibres is perpendicular to the longitudinal axis. At the ends of the beams, this effect is not as strong, owing to the end plates of the formwork (*Fig. 8*).

In the case of method P1, the mean value (of the number of intersecting fibres) for the synthetic fibres was 9.1% higher than that for the steel fibres while for method P2, the values were almost similar. The M-estimator values for the synthetic fibres for P1 and P2 were 13.1% and 16.4% higher, respectively, than those for the steel fibres. Moreover, for the same pouring method, in almost all the cases, more synthetic fibres were observed in the cross-section than the steel fibres. This is in contradiction to the results of the proposed analytical model, since according to the model, the total orientation factor is higher in the case of the steel fibres and would result in more steel fibres intersecting the cross-section.

The normality test results suggested that the following data for the synthetic fibres exhibited a normal distribution: method P1 and the entire cross-section and method P2 and all the zones as well as the entire cross-section. In contrast, for the steel fibres, only the data for zone Z3 for both pouring methods and those for zone Z2 and method P1 exhibited a normal distribution. However, the number of samples in the corner zone, that is, Z3, is not as relevant, given the small area of the zone. Thus, if the data for the entire cross-section were not normal, the normality of the data for Z3 was probably incorrect. In summary, the null hypothesis, namely, that the distribution of the data were normal, was accepted only in the case of the synthetic fibres. This conclusion can be confirmed through a visual inspection of the histograms: in case of the steel fibres, the distributions were either asymmetrical or bimodal.

The CV values for the different cross-section zones lay between 31.8% and 56.6% in the case of the steel fibres and between 14.7 and 52.1% in the case of the synthetic fibres. Further, the CV values for the entire cross-section lay between 32.3% and 35.2% in the case of the steel fibres and between 14.7% and 24.2% in the case of the synthetic fibres, meaning that the distributions of the synthetic fibres in the beams were slightly more uniform.

On comparing the results of the proposed analytical model with those of the laboratory tests, the following conclusions could be drawn. The orientation factors obtained using the analytical model closely approximated the M-estimator values for the steel fibres and method P1, while in the case of the synthetic fibres, the closest estimates were the mean values in the case of method P2. The orientation factor of the analytical model for the corner zone (Z3) yielded the worst estimates in all the cases: in the case of the steel fibres, the orientation factors for zone Z3 were the lowest, in contrast to the predictions of the model. On the other hand, in the case of the steel fibres, the analytical model results differed significantly from the test results: the undisturbed zone (Z1) exhibited the highest orientation factor, while the zones with the wall effect (Z2 and Z3) exhibited smaller values. Although, in the case of the steel fibres, there is an upper limit for fibre content. Above this limit, the effect of the fibres on their respective movements should also be taken into account, as this would result in more of the fibres being located in the middle zone than in the edge and corner zones (Juhász, 2018b; Czoboly, 2016). The actual concentration of 33.73 kg/m^3 was higher than this limit. With respect to this steel fibre concentration, which is used widely in the industry, the standard cross-section dimensions of 150 × 150 mm^2 seem to be insufficient for the steel fibres in question.

Based on the results of the statistical analysis and after comparing the test and analytical results, the following conclusions can be drawn. In case of steel fibres, the use of the M-estimator is recommended, given the significant divergence of the data from a normal distribution. Further, the analytical model is suitable in the case of pouring method P1. In case of synthetic fibres, the analytical model underestimates the orientation factors for P1 and overestimates them for P2. However, it yields good estimates of the average values for the two pouring methods. According to the analytical model, there is no significant difference between the orientation factors of the undisturbed zone (Z1) and the edge zone (Z2). This was confirmed in the case of pouring method P1 but not in the case of pouring method P2.

According to the obtained results, the wall effect affects the orientation factors to a lesser degree than the flow type and direction of the concrete. Consequently, knowing the flow type and direction of the concrete and taking these factors into account during the modelling of FRC is of greater importance.

As per this study, the mean value of the orientation factors related to the different flow directions will lie between 0.3 and 0.6. Thus, 0.5 seems to be a good value to assume. Finally, the assumption of the existence of different cross-section zones seems to be invalid in most cases. This is true for both steel and synthetic fibres.

6. CONCLUSIONS

The residual tensile strength of FRC depends primarily on the number of fibres that intersect the cracked cross-section of the structure in question. While the mixing of the fibres should ideally be uniform, this is not the case in reality, owing to various factors. In this study, the effects of the pouring method on the orientation factors of steel and synthetic fibres were investigated. Beams were produced using two different pouring methods, and the orientation factors in the different zones of sections of these beams were investigated. The obtained results were compared with the orientation factors reported in the literature.

The study examined two types of fibres: steel and synthetic. The dosage of these fibres was chosen so that the number of mixed fibres was the same. In this study, the matrix of fibre-reinforced concrete was kept constant, while the pouring method varied. Moreover, the orientation of the fibres can be affected by a number of parameters, which were not detailed in this study, e.g., fibre length and shape, aggregate type and size, paste saturation, etc. These parameters may have varying degrees of influence on the orientation factors, which can be elucidated in future studies.

According to the results obtained in this study, there is a difference of 34–40% in the orientations, based on the pouring method used. This difference is significant and must be taken into account during the engineering design stage. In the case of the standard beams used for tests, owing to the vibrations that occur during the manufacturing of the test specimens, the fibres are oriented along the longitudinal axis of the beams. As a result, more fibres intersect the cross-section than would be the case for a uniform distribution. In the case of flowable concrete, the fibres are oriented perpendicular to the flow direction. Thus, fewer fibres intersect the cross-section that would be the case if the flow were parallel to the longitudinal axis of the beam. Thus, the error may be magnified in that the material parameters may be overestimated, although in the sections of actual structures, the number of fibres intersecting the cross-section may also be overestimated if their orientation is unsuitable. Thus, there can be a significant difference between the tension or moment capacities as calculated based on the overestimated material parameters and the actual capacity of the structure.

Thus, in the case of precast elements and structures that are functionally important, the orientation of the reinforcing fibres added to the concrete must be considered during the design stage.

7. REFERENCES

Alberti, M.G., Enfedaque, A. and Gálvez, J.C. (2017), „On the prediction of the orientation factor and fibre distribution of steel and macro-synthetic fibres for fibre-reinforced concrete", *Cement and Concrete Composites* 77, pp. 29–48, https://doi.org/10.1016/j.cemconcomp.2016.11.008

ASTM C1609 (2019), „Standard test method for flexural performance of fiber-reinforced concrete (Using beam with third-point loading)", ASTM International, West Conshohocken, PA, 2019, www.astm.org, https://doi.org/10.1520/C1609_C1609M-19

Balaguru, P.N. and Shah, S.P. (1992), „Fiber reinforced cement composites", *McGraw-Hill International Editions, Civil Engineering Series*

Barragán, B.E., Gardner, D., Gettu, R. and Ferreira, L.E.T. (2000), „Study of the distribution and orientation of fibers in cast cylinders", Report for Test and Deisng Methods for Steel Fibre Reinforced Concrete, EU Contract–BRPR–CT98-813.

Bernard, E.S. (2013), „Development of a 1200-mm-diameter round panel test for post-crack assessment of fiber-reinforced concrete," *Advances in Civil Engineering Materials* 2(1), pp. 457–471, https://doi.org/10.1520/ACEM20120021

Chasioti, S. (2017), „*Hybrid steel fibre reinforced concrete in shear: from the material to the structural level*", Doctoral thesis, University of Toronto, Toronto, 2017.

CNR-DT 204/2006 (2006), „*Guide for the Design and Construction of Fiber-Reinforced Concrete Structures*", design recommendation, Advisory Committee on Technical Recommendations for Construction, CNR, Rome

Czoboly O. (2016), „A keverési idő és a keverési mód hatása a szálak és a szálerősítésű betonok jellemzőire (The effect of mixing time and mixing mode on the characteristics of fibres and fibre reinforced concrete, in Hungarian)", Doctoral thesis, Budapest University of Technology and Economics, Budapest.

Dupont, D. and Vandewalle, L. (2005), „Distribution of steel fibres in rectangular sections", *Cement & Concrete Composites* 27, pp. 391–398, https://doi.org/10.1016/j.cemconcomp.2004.03.005

Edgington, J. and Hannant, D. J. (1972), „Steel Fibre Reinforced Concrete. The effect on fibre orientation of compaction by vibration", *Materials and Structures* 5(25), pp. 41–44, https://doi.org/10.1007/BF02479076

EN 14651 (2007), „Test method for metallic fibre concrete – measuring the flexural tensile strength (limit of proportionality (LOP), residual)", European Committee for Standardization, https://doi.org/10.3403/30092475

fib (2013), „Model Code for Concrete Structre 2010", *Wiley Erst & Sohn*.

Gopalaratnam, V.S., Shah, S.P., Batson, G.B., Criswell, M.E., Ramakrishnan, V. and Wecharatana, M. (1991), „Fracture toughness of fiber reinforced concrete", *ACI Materials Journal* 88(4), pp. 339–353, https://doi.org/10.14359/1840

Hoy, C.W. (1998), „Mixing and mix proportioning of fibre reinforced concrete", Doctoral thesis, Department of Civil, Structural and Environmental Engineering, University of Paisley, Scotland, 284 p.

Juhász K.P. (2013), „Szintetikus makro szálerősítandű beton gerendavizsgálatok kiértékelande a valós száleloszlás vizsgálata alapján (Evaluation of synthetic macro fibre reinforced concrete beam test results based on the examination of the real fibre distribution, in Hungarian)", Anyagvizsgálók Lapja 23, pp. 93–97.

Juhász, K.P. (2015), „Evaluation of fibre reinforced concrete beam test results based on the examination of the real fibre distribution", in: A. Kohoutková et al. (Eds.), *Proceedings of Fibre Concrete 2015*. Prague, Czech Republic.

Juhász K. P. (2018a), „Acél and szintetikus szálak orientációjának meghatározása szálerősítésű betonban (Determining the orientation of steel and synthetic fibres in fibre reinforced concrete, in Hungarian)", Építés-Építészettudomány 46(1–2), pp. 221–238, https://doi.org/10.1556/096.2017.007

Juhász K. P. (2018b) „The effect of synthetic fibre reinforcement on the fracture energy of the concrete", Doctoral thesis, Budapest University of Technology and Economics, Budapest, https://perma.cc/4JMY-HN5C

Juhász K.P. (2019), „Analytical model for rigid (steel) and flexible (synthetic) fibre mixing in concrete", IOP Conference Series: Materials Science and Engineering 596, https://doi.org/10.1088/1757-899X/596/1/012003

Kameswara Rao, C.V.S. (1979), „Effectiveness of random fibres in composites", *Cement and Concrete Research* 9, pp. 685-693, https://doi.org/10.1016/0008-8846(79)90063-2

Kang, S.T., Lee, B.Y., Kim, J-K., Kim, Y.Y. (2011), „The effect of fibre distribution characteristics on the flexural strength of steel fibre-reinforced ultra high strength concrete", *Construction and Building Materials* 25(5), pp. 2450–245, https://doi.org/10.1016/j.conbuildmat.2010.11.057

Kooiman, A.G. (2000), „Modelling steel fibre reinforced concrete for structural design", Doctoral thesis, Technical University of Delft (The Netherlands), pp. 87–106.

Krenchel, H. (1975), „Fibre spacing and specific fibre surface", A. Neville, (ed.) *Fibre reinforced cement and concrete*, London: The Construction Press, pp. 67–75.

Lee, S.C., Cho, J.Y., and Vecchio, F. J. (2011), „Diverse Embedment Model for Steel Fiber-Reinforced Concrete in Tension: Model Development", *ACI Materials Journal* 108(5), pp. 516–525, https://doi.org/10.14359/51683261

Lee, S.C., Cho, J.Y., Vecchio, F.J. (2013) „Simplified diverse embedment model for steel fiber-reinforced concrete elements in tension", *ACI Materials Journal* 110, pp. 403–412.

Naaman, A. E. (1972), „A statistical theory of strength for fiber reinforced concrete", Doctoral thesis, Massachusetts Institute of Technology.

Ng, T.S., Foster, S.J. and Htut T.N.S. (2012), „Fracture of Steel Fibre Reinforced Concrete – the Unified Variable Engagement Model", UNICIV Report R–460, School of Civil and Environmental Engineering, The University of New South Wales.

Oh, B.H., Kim, J.C. and Choi, Y.C. (2007), „Fracture behavior of concrete members reinforced with structural synthetic fibers", *Engineering Fracture Mechanics* 74, pp. 243–257, https://doi.org/10.1016/j.engfracmech.2006.01.032

Österreichusche Vereinigung für Beton- und Bautechnik (2008), „Richtlinie Faserbeton", Vienna.

Romualdi, J.P. and Mandel, J.A. (1964), „Tensile strength of concrete affected by uniformly distributed and closely spaced short lengths of wire reinforcement", *Journal of the American Concrete Institute* 61(6), pp. 657–671, https://doi.org/10.14359/7801

Sarmiento, E. V., Zirgulis, G., Sandbakk, S., Geiker, M. R. and Kanstad, T. (2012), „Influence of concrete flow on fibre distribution, orientation and mechanical properties of fibre reinforced concrete", in J. Barros (ed) *BEFIB2012 – Fibre reinforced concrete*

Stahli, P. and van Mier, J.G.M. (2007), „Effect of Manufacturing Methods on Tensile Properties of Fibre Concrete", in *Proceedings of Fracture Mechanics for Concrete and Concrete Structures (FraMCos)6*, Catania, Italy.

Stahli, P., Custer, R. and van Mier, J.G.M., (2008), „On flow properties, fibre distribution, fibre orientation and flexural behaviour of FRC", *Materials and Structures* 41(1), pp. 189–196, https://doi.org/10.1617/s11527-007-9229-x

Stroeven, P. (1978), „Morphometry of fiber reinforced cementitious materials", *Materials and Structures* 11(61), pp. 31–37, https://doi.org/10.1007/BF02478701

Stroeven, P. (1979), „Morphometry of Fibre Reinforced Cementitious Materials, Part II: Inhomogenity, segregation and anisometry of partially oriented fibre structures", *Materials and Structures* 12(67) pp. 9–20, https://doi.org/10.1007/BF02473994

Stroeven, P. (1991), „Effectiveness of steel wire reinforcement in a boundary layer of concrete", *Acta Stereol* 10(1), pp.113–22.

Stroeven, P. (1999), „Steel fibre reinforcement at boundaries in concrete elements", in *Proceedings of the Third International Workshop on High Performance Fiber Reinforced Cement Composites (HPFRCC3)*, Mainz (Germany), pp. 413–421.

Soroushian, P. and Lee, C. (1990), „Distribution and orientation of fibers in steel fiber reinforced concrete", *ACI Mater Journal* 87(5), pp. 433–439, https://doi.org/10.14359/1803

Toutanji, H. and Bayasi, Z. (1998), „Effects of Manufacturing Techniques on the Flexural Behavior of Steel Fiber-Reinforced Concrete", *Cement and Concrete Research* 28(1), pp. 115–124, https://doi.org/10.1016/S0008-8846(97)00213-5

Vandewalle, L. et al. (2003), „RILEM TC 162-TDF: Test and design methods for steel fibre reinforced concrete – σ-ε design method", *Materials and Structures* 36(8), pp. 560–567, https://doi.org/10.1617/14007

Voo, J. Y. L.; Foster, J.S. (2003), „Variable engagement model for the design of fibre reinforced concrete structures", in: V. Mistry et al., (Eds.) *Advanced Materials for Construction of Bridges, Buildings, and Other Structures III.* Davos, Switzerland, 2003, pp. 1–10.

Zerbino, R., Tobes J. M., Bossio M. E. and Giaccio G. (2012), „On the orientation of fibres in structural members fabricated with self compacting fibre reinforced concrete", *Cement & Concrete Composites* 34, pp. 191–200, https://doi.org/10.1016/j.cemconcomp.2011.09.005

Károly Péter Juhász (1980), Structural Engineer MSc., PhD, owner and chief engineer of JKP Static Ltd. His main fields of activities are experimental investigation and modelling of synthetic fibre reinforced concrete, finite element modelling of concrete structures. He is a member of the Hungarian Group of ***fib*** and the ***fib*** Working Group 2.4.2. email: office@jkp.hu